

Identifying true satellites of the Magellanic Clouds

Laura V. Sales,¹★ Julio F. Navarro,²† Nitya Kallivayalil³ and Carlos S. Frenk⁴

¹*Department of Physics and Astronomy, University of California Riverside, 900 University Avenue, CA 92507, USA*

²*Department of Physics and Astronomy, University of Victoria, Victoria, BC V8P 5C2, Canada*

³*Department of Astronomy, University of Virginia, Charlottesville, VA 22904, USA*

⁴*Institute for Computational Cosmology, Department of Physics, University of Durham, South Road, Durham DH1 3LE, UK*

Accepted 2016 October 31. Received 2016 October 29; in original form 2016 May 7

ABSTRACT

The hierarchical nature of Λ CDM suggests that the Magellanic Clouds must have been surrounded by a number of satellites before their infall into the Milky Way halo. Many of those satellites should still be in close proximity to the Clouds, but some could have dispersed ahead/behind the Clouds along their Galactic orbit. Either way, prior association with the Clouds constrains the present-day positions and velocities of candidate Magellanic satellites: they must lie close to the nearly polar orbital plane of the Magellanic Stream, and their distances and radial velocities must follow the latitude dependence expected for a tidal stream with the Clouds near pericentre. We use a cosmological numerical simulation of the disruption of a massive sub-halo in a Milky Way-sized Λ CDM halo to test whether any of the 20 dwarfs recently discovered in the Dark Energy Survey, the Survey of the Magellanic Stellar History, Pan-STARRS, and ATLAS surveys are truly associated with the Clouds. Of the six systems with kinematic data, only Hor 1 has distance and radial velocities consistent with a Magellanic origin. Of the remaining dwarfs, six (Hor 2, Eri 3, Ret 3, Tuc 4, Tuc 5, and Phx 2) have positions and distances consistent with a Magellanic origin, but kinematic data are needed to substantiate that possibility. Conclusive evidence for association would require proper motions to constrain the orbital angular momentum direction, which, for true Magellanic satellites, must be similar to that of the Clouds. We use this result to predict radial velocities and proper motions for all new dwarfs, assuming that they were Magellanic satellites. Our results are relatively insensitive to the assumption of first or second pericentre for the Clouds.

Key words: galaxies: evolution – galaxies: formation – galaxies: haloes – galaxies: kinematics and dynamics.

1 INTRODUCTION

The Large and Small Magellanic Clouds (LMC and SMC, respectively) are a galaxy pair orbiting together in the halo of the Milky Way (MW) and provide a prime example of the nested hierarchy of structures expected in the Λ CDM galaxy formation paradigm (Springel et al. 2008b). Their physical association seems beyond doubt, given their relative proximity, correlated kinematics, and abundant evidence of past interaction (for a recent review, see e.g. D’Onghia & Fox 2016).

The path of the Clouds around the Galaxy is well constrained by precise estimates of their distances, positions, radial velocities and proper motions, which indicate a nearly polar orbit on a plane closely aligned with the Magellanic Stream (Kallivayalil et al. 2006). The Clouds are just past pericentre, since their

Galactocentric radial velocities are positive and much smaller than their tangential velocities ($V_t \sim 314 \text{ km s}^{-1}$, $V_r \sim +64 \text{ km s}^{-1}$ for the LMC; see e.g. Kallivayalil et al. 2013). Their orbit must also have a fairly large apocentric radius, since their total speed ($|V_{\text{LMC}}| \sim 321 \text{ km s}^{-1}$) exceeds the circular velocity of the MW ($\sim 220 \text{ km s}^{-1}$) by a substantial amount. A large apocentre implies a long orbital period, which has led to the suggestion that the Clouds might be on their first pericentric passage.

This conclusion depends on the total mass assumed for the MW halo, as well as on its assumed outer radial profile (Besla et al. 2007), but it would explain naturally why the LMC and SMC are still so tightly bound. Indeed, if the Clouds were at first pericentre then the Galactic tide would not have yet had time to disrupt the pair nor to disperse fully the common (sub-)halo they inhabit. As a result, most other dwarf companions of the Clouds should still lie in their close vicinity. Such ‘Magellanic satellites’ have long been speculated (see e.g. Lynden-Bell & Lynden-Bell 1995), and their existence would be consistent with the relatively common occurrence of dwarf galaxy associations in the nearby Universe (Tully et al. 2006). The

* E-mail: lsales@ucr.edu

† Senior CIFAR Fellow.

immediate surroundings of the Clouds should thus be fertile ground to search for new dwarfs, as proposed by Sales et al. (2011, S11 hereafter).

A full search for satellites around the Clouds would be extremely valuable. One reason is that, in Λ CDM, the satellite luminosity function is expected to be a nearly scale-free function when expressed in units of the luminosity of the primary (Sales et al. 2013). In other words, to first order, the Galactic satellite abundance should be simply a scaled-up version of that of the Clouds. A complete catalogue of Magellanic faint and ultra-faint satellites would be easier to compile (the relevant survey volume is much smaller than the full Galactic halo) and could therefore help to constrain the incompleteness of all-sky surveys of Galactic satellites. In general, the surrounding of dwarf galaxies, especially those in the field, are promising sites for the discovery of new faint galaxies (Sales et al. 2013; Wheeler et al. 2015).

A second application would be to clarify the effects of environment on the star formation history of dwarfs (D’Onghia & Lake 2008; Wetzel, Deason & Garrison-Kimmel 2015). An unambiguous identification of Magellanic origin would enable a direct comparison with Galactic satellites of similar stellar mass that have evolved in a rather different environment. Finally, Magellanic satellites might also provide clues to the nature of dark matter: indeed, fewer satellites are expected around the MW in general, and the LMC in particular, if dark matter was ‘warm’ rather than cold (see e.g. Kennedy et al. 2014).

Given this context, it is not surprising that the recent discovery of a number of candidate dwarfs in southern surveys targeting the Clouds’ vicinity, such as the Dark Energy Survey (DES; Bechtol et al. 2015; Drlica-Wagner et al. 2015; Kim & Jerjen 2015; Kim et al. 2015a; Koposov et al. 2015b), the Survey of the Magellanic Stellar History (SMASH; Martin et al. 2015), as well as in other large surveys, such as PAN-STARRS (Laevens et al. 2015), and ATLAS (Torrealba et al. 2016), have attracted much attention.

While not all of these candidates have follow-up spectroscopy confirming that they are dark matter-dominated dwarf galaxies rather than star clusters—six have spectra thus far (Kirby, Simon & Cohen 2015; Martin et al. 2016; Walker et al. 2016)—they do occupy the same region in the size–luminosity plane as ultra-faint dwarf galaxies (M_V between -2.0 and -7.8 and half-light radii, r_h , between ~ 18 and ~ 1000 pc). It is not clear either which of these dwarfs, if any, have a Magellanic origin.

On that point, Deason et al. (2015) cite a statistical argument based on abundance-matching models applied to massive sub-halos in the ELVIS simulations (Garrison-Kimmel et al. 2014) to suggest that 2–4 of the 9 then known DES candidates might have come into the MW with the LMC. Yozin & Bekki (2015), on the other hand, conclude, on the basis of orbit models, that the majority of the DES dwarfs could have been at least loosely associated with the Clouds. Yet another analysis suggests, using tailor-made numerical simulations, that only about half of the DES new dwarf galaxies are very likely to have been associated with the LMC in the past (Jethwa, Erkal & Belokurov 2016).

Here, we take a complementary and targeted approach, using an LMC analogue sub-halo identified in a fully cosmological simulation of an MW-sized halo in Λ CDM. We track the positions and velocities of sub-halo particles to constrain the likely location in phase space of systems with prior association with the Clouds. This is an extension of the analysis previously presented in S11, who concluded that *none* of the 26 MW satellites known at the time were convincingly associated with the Clouds. The main goal of the present work is to assess the likelihood of association with the

Clouds of the recently discovered dwarfs, as well as to predict the radial velocities and proper motions required for that association to be true.

In Section 2, we describe our numerical setup; in Section 3, we present the main results, including the expected sky distribution of the companion dwarfs, their radial velocities, likelihood of association with the LMC, as well as their 3D orbits. We conclude with a brief summary of our main conclusions in Section 4.

2 NUMERICAL SIMULATIONS

We use the Aquarius Project (Springel et al. 2008a), a suite of zoomed-in cosmological simulations that follow the formation of six MW-sized haloes with virial¹ masses in the range $0.8\text{--}1.8 \times 10^{12} M_\odot$. These haloes were selected from a large-scale simulation of a cosmologically representative volume (the Millennium-II Simulation; see Boylan-Kolchin et al. 2009). The assumed cosmology is characterized by the following parameters: $\Omega_m = 0.25$, $\Omega_\Lambda = 0.75$, $\sigma_8 = 0.9$, $n_s = 1$, and Hubble constant $H_0 = 100 h \text{ km s}^{-1} \text{ Mpc}^{-1} = 73 \text{ km s}^{-1} \text{ Mpc}^{-1}$, consistent with WMAP1 and WMAP5 data (Spergel et al. 2003; Komatsu et al. 2009). We focus in this paper on the properties of an ‘LMC analogue’ system (hereafter identified as LMCa, for short) which was identified and presented in S11.

2.1 LMCa: the LMC analogue

LMCa was chosen because it is a fairly massive sub-halo with a pericentric distance (~ 50 kpc) and velocity ($\sim 400 \text{ km s}^{-1}$) in good agreement with that of the LMC (Kallivayalil et al. 2006, hereafter K06). Identified before first infall (defined here as the time when the LMCa reaches its maximum mass), at $z_{\text{id}} = 0.9$, LMCa has a virial mass of $M_{200} = 3.6 \times 10^{10} M_\odot$, which corresponds to a circular velocity of $\sim 65 \text{ km s}^{-1}$. The LMCa system has a mass lower than expected for the real LMC, either from abundance-matching arguments, $M_{200} \sim 3 \times 10^{11} M_\odot$ (Behroozi, Wechsler & Conroy 2013; Moster, Naab & White 2013), or from recent measurements of its circular velocity, $V_{\text{cir}} \sim 91.7 \pm 18.8 \text{ km s}^{-1}$ (van der Marel & Kallivayalil 2014). The difficulty to find a better suitable candidate for our analysis comes from the rarity of the Clouds: they seem quite massive compared to the mass of the MW and are also on a rare orbit (Boylan-Kolchin, Besla & Hernquist 2011). We proceed with our analysis in what follows, correcting for the mass of our LMCa by a factor of $8.3 = 3.0 \times 10^{11} / 3.6 \times 10^{10}$ when necessary (see Section 3.4).

LMCa first crosses the virial boundary of the main Aquarius halo (Aq-A) at $z = 0.51$ ($t = 8.6$ Gyr), reaches first pericentre at $t_{1p} = 9.6$ Gyr, and is able to complete a second pericentric passage at $t_{2p} = 13.3$ Gyr. (These times are actually slightly past actual pericentre, thus chosen so as to best accommodate the fact that the LMC has a slight positive radial velocity and is itself just past pericentre at present.) The host halo has a virial mass of $M_{200} = 1.8 \times 10^{12} M_\odot$ at $z = 0$ and $M_{200} = 1.4, 1.6 \times 10^{12} M_\odot$ at t_{1p} and t_{2p} , respectively, which agree well with the upper end of current MW mass estimates (e.g. Smith et al. 2007; Li & White 2008; Boylan-Kolchin et al. 2013; McMillan 2016).

¹ We define the virial mass, M_{200} , as that enclosed by a sphere of mean density 200 times the critical density of the Universe, $\rho_{\text{crit}} = 3H^2/8\pi G$. Virial quantities are defined at that radius, and are identified by a ‘200’ subscript.

At t_{1p} and t_{2p} , the distances, radial velocities, and tangential velocities are, respectively, $r_{1p} = 65$ kpc, $r_{2p} = 69$ kpc, $V_{r,1p} = 78$ km s⁻¹, $V_{r,2p} = 89$ km s⁻¹; $V_{t,1p} = 345$ km s⁻¹; and $V_{t,2p} = 302$ km s⁻¹. These values are in reasonable agreement with the K06 LMC measurements (see fig. 1 in S11), although the tangential velocities are a bit below the observed values. The revised proper motions for the LMC from Kallivayalil et al. (2013) suggest a slightly lower total velocity than previously determined, 321 ± 24 km s⁻¹ compared to 378 ± 31 km s⁻¹, resulting from the combination of an added third epoch of observations, the adoption of a different local standard of rest, and a new determination of the LMC’s dynamical centre. This decrease in velocity accommodates the tangential motion of LMCa more comfortably at both pericentres.

It is still a matter of debate whether the Clouds are on the first or the second pericentric passage (see e.g. Shattow & Loeb 2009, S11), although indirect evidence favours a first infall scenario, including (i) their large tangential velocity, (ii) their blue colours and large gas content, and (iii) the requirement that the LMC and SMC have been a long-lived binary (which favours a low-mass MW, or a high-mass LMC; see discussion in Kallivayalil et al. 2013). Therefore in what follows we analyse in detail a first infall scenario but include a brief discussion about how our conclusions would be affected if the LMC is in its second pericentre passage (Section 3.5).

Following S11, we use the Aquarius ‘A’ halo at level 3 resolution, or Aq-A-3 in the notation of Springel et al. (2008a), which has a mass per particle $m_p = 4.9 \times 10^4 M_\odot$ and a spatial resolution $\epsilon = 120.5$ pc. We identify and follow all particles that were associated with the LMCa friends-of-friends group at the time of infall (i.e. at z_{id}), and evaluate their positions and velocities at the time of the first and second pericentre passages.

Using SUBFIND (Springel, Yoshida & White 2001), we have identified more than 200 sub-halos associated with LMCa at infall time (see fig. 1 in S11 for their individual orbits), confirming our expectation that a large satellite such as the LMC should bring along its own population of satellites (Springel et al. 2008b).

We use for our analysis *all* particles (and not just the sub-halos) initially bound to LMCa in order to provide a more complete sampling of the positions and velocities of any potential companion associated with the LMC. Dark matter-only simulations indicate that sub-halos have a shallower radial distribution than the dark matter in the host, showing a suppressed presence within $r/r_{200} \sim 0.2$ – 0.5 (e.g. Diemand, Moore & Stadel 2004; Gao et al. 2004). Encouragingly, however, simulations that include the presence of baryons show an improved agreement between the distribution and kinematics of satellites and the dark matter host halo, showing little systematic differences outside $0.1r_{200}$ (Sales et al. 2007; Vogelsberger et al. 2014). This is in nice agreement with observational results from large stacking of satellites in Sloan Digital Sky Survey (see discussion in section 1 of Wang et al. 2014). Assuming that rotation speed equals its virial velocity, we estimate a virial radius for the LMC of $r_{200} \sim 130$ kpc. It is therefore reasonable to use dark matter particles as tracers of satellite properties as far as we stay beyond ~ 13 kpc from the LMC. All newly discovered faint dwarfs analysed here are more distant from the LMC than such threshold, with the closest one being Ret 2 at ~ 24 kpc.

2.2 Lmca in Galactic coordinates

We transform the coordinate system of the simulation into ‘Galactic coordinates’ by requiring that the orientation of the orbital angular momentum of LMCa coincides with that measured for the LMC’s orbit, and that its position on the sky coincides with the LMC. For

consistency with S11, we use throughout this paper the LMC proper motion as given by K06.² After the rotation, we also rescale slightly all Galactocentric distances (so that LMCa is, at each pericentre, at the measured distance of the LMC 49 kpc). For this we apply a small inward shift, 16.5 and 19.8 kpc for the first and second pericentre passages, respectively, to all particles in our LMCa, leaving their velocities unchanged. This effectively places the centre of our LMCa at the exact same position of the LMC today.

3 RESULTS

We first examine the sky distribution of particles associated at infall with the LMC analogue sub-halo (hereafter ‘LMCa debris’, for short). We use this footprint, as well as their radial and tangential velocities, to compare with available data for the newly discovered dwarfs. As mentioned above, we shall interpret coincidence in sky position, radial velocity, and distance between debris particles and observed dwarfs as evidence of a possible association with the LMC.

3.1 Lmca debris: sky distribution and distances

At the time of the first pericentre, tidal disruption due to the host halo has already set in, but most particles are still bound and close to the sub-halo centre. The rest of the material is distributed along a thick but well-defined tidal stream that follows the projection of the sub-halo’s orbital path on the sky. A leading and trailing arm extends towards more positive and negative latitudes, respectively. The distribution of this debris roughly agrees with the position of the H I Magellanic Stream, sketched here by a line that traces the high-density H I in the sky maps of Nidever et al. (2010).

Most of the debris, however, is close to the current position of the Clouds (grey squares indicate the observed positions of the LMC and SMC). Particles are colour coded in Fig. 1 by their Galactocentric distance (see colour bar), which shows a clear gradient along the stream with distances reaching up to 300 kpc, well beyond the virial radius of the main host.

For reference, we indicate the positions of all known MW satellites in the figure as well. Red-filled circles correspond to the ‘classical’ (i.e. brighter than $M_V = -8$) dwarf spheroidal (dSph) companions of the MW; open circles indicate the position of previously known, fainter satellites. We refer the interested reader to S11 for a discussion of the likelihood of association with the LMC of those satellites.

The recently discovered dwarfs that are the focus of this paper are shown using black-starred symbols in Fig. 1. We include in this sample: (i) the dwarfs reported by Kozlov et al. (2015b) from year-1 DES data (see also Bechtol et al. 2015), (ii) the six certain detections from year-2 DES data (Drlica-Wagner et al. 2015), and (iii) additional individual discoveries such as Hydra II (Hy II; Martin et al. 2015), Horologium 2 (Hor 2; Kim & Jerjen 2015), Pegasus 3 (Peg 3; Kim et al. 2015a), Draco 2 and Sagittarius 2 (Dra 2 and Sag 2; Laevens et al. 2015), and Crater 2 (Cra 2; Torrealba et al. 2016). Table 1 lists all the ‘new dwarfs’ considered in what follows (i.e. black stars in Fig. 1). With the exception of Hy II, Cra

² We note however that the change in the direction of the orbit given by the new updated measurements from Kallivayalil et al. (2013) is very small: $(j_x, j_y, j_z) = (-0.97, 0.14, -0.18)$ versus $(-0.98, 0.11, -0.13)$ for the 2006 and 2013 determinations, respectively. These numbers correspond to a unit vector in a Cartesian system aligned with the disc of the galaxy, as described in Section 3.

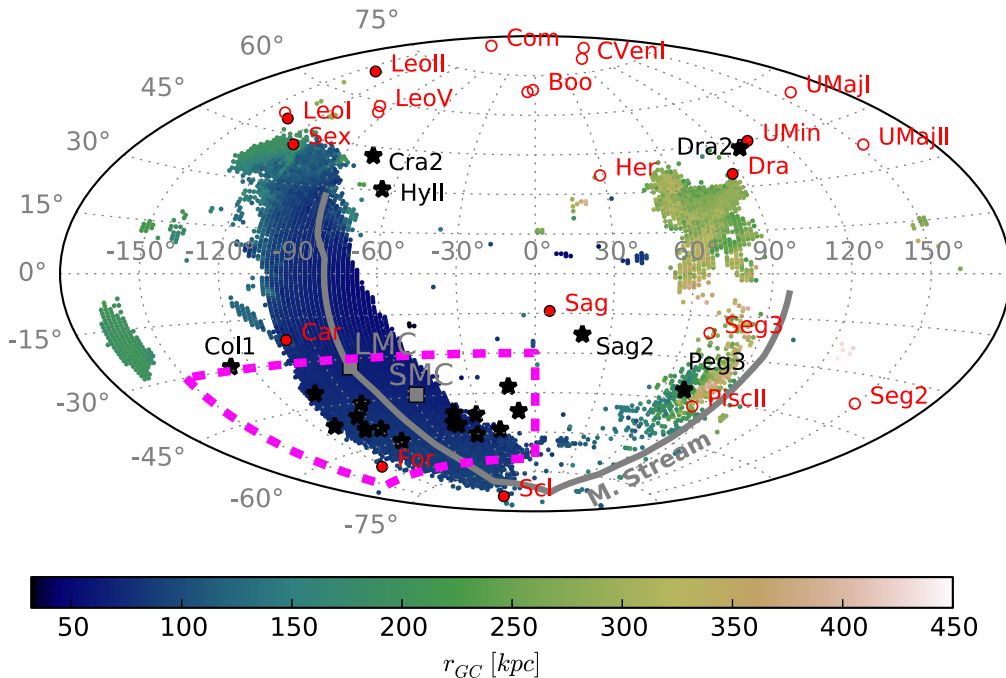


Figure 1. Aitoff projection of particles associated with the LMC analogue sub-halo (LMCa), shown just after first pericentric approach, when its pericentric distance and velocity closely matches that of the Large Magellanic Cloud. The LMCa centre is chosen to coincide with the LMC and coordinates are chosen so that the direction of its orbital angular momentum matches that of the LMC. This results in a nearly polar orbital plane which roughly aligns with the Magellanic Stream (grey line). Particles of the LMC analog (identified before infall) are coloured by their average Galactocentric distance. Red circles indicate the position of known Milky Way satellites. Filled circles indicate ‘classical’ dwarf spheroidals (i.e. brighter than $M_V = -8$); open circles denote fainter objects. Newly discovered dwarfs (the subject of this paper) are shown as black-starred symbols. The magenta dashed line indicates the region of the sky to be zoomed-in in Fig. 2.

2, and Dra 2, all other dwarfs are in the region of the sky occupied by the trailing arm of the stream.

Fig. 1 shows that position on the sky and distance provide on their own powerful constraints on a potential Magellanic origin for a dwarf. Those satellites must be close to the orbital plane (traced by the debris and the Magellanic Stream), ruling out satellites like Sagittarius, Hercules, and Seg 2. In addition, the farther a satellite is from the LMC the larger, on average, its Galactocentric distance should be, a fact that rules out many of the satellites in the Galactic northern cap. Indeed, the latter are typically much closer to the Galactic Centre than the leading arm of the LMCa debris, which reaches a distance of ~ 180 kpc at $b = +45^\circ$.

Fig. 2 zooms in on the vicinity of the LMC (the region highlighted by the magenta box in Fig. 1) and shows in more detail the position of individual dwarfs as well as the distance gradient expected for this section of the stream. This figure also shows that Col 1 lies outside of the LMCa debris footprint. This, combined with its large distance (~ 182 kpc), makes a Magellanic association rather unlikely (see also Drlica-Wagner et al. 2015). We therefore exclude Col 1 from the rest of our analysis, together with Sag 2, whose position in the sky is not favourable either. Furthermore, we also remove Indus 1 from our analysis since it has now been classified as a stellar cluster rather than as a dwarf galaxy (Kim et al. 2015b).

The distance gradients with Galactic latitude shown in Fig. 1 and 2 result from the fact that LMCa is close to pericentre and, therefore, at roughly the minimum distance of all associated debris. Debris north of the LMC is farther away and moving out (already past pericentre), whereas debris to the south is also farther away but moving in (has yet to reach pericentre). This induces a correlated signature in the radial velocities, which we explore next.

3.2 Lmca debris: radial velocities

We explore the correlation between radial velocity and Galactic latitude in Fig. 3. This figure shows the Galactocentric radial velocity V_r as a function of distance r_{GC} for LMCa debris in the Galactic longitude range $l = [210^\circ - 360^\circ]$, which encloses the stream and the positions of the DES dwarfs. To convert heliocentric velocities to radial velocities for the observed dwarfs, we assume the velocity of the Sun as determined by Dehnen & Binney (1998), $(U_\odot, V_\odot, W_\odot) = (10.0, 225.2, 7.2)$ km s $^{-1}$.

Particles are coloured according to their Galactic latitude, in the range $-80^\circ < b < 0^\circ$ (see colour bar). Fig. 3 shows a clear gradient in radial velocity with Galactic latitude, showing generally positive values (outward moving) for particles north of the position of the LMC (i.e. $b_{LMC} > -32.9^\circ$) and negative values (infalling) for those south of that. Although the latitude trend is clear, the dispersion about the mean trend is quite large. This is because the velocity dispersion of LMCa before infall was quite substantial (at $z_{id} = 0.9$, $\sigma_{200} = V_{200}/\sqrt{2} = 44.5$ km s $^{-1}$), making the tidally induced stream quite thick. As a result, the constraints on a possible Magellanic origin provided by b , r_{GC} , and V_r alone are relatively lax, and serve mainly to rule out the most unlikely candidates.

For example, Fig. 3 shows that Fornax (even though it is close to the stream in sky projection) has a distance that is too large to be associated with the LMC, whereas the SMC, as expected, lies well within the velocity-distance range spanned by the LMCa debris. Starred symbols show the ‘new dwarfs’ that fall in this region of the sky and for which kinematic measurements are available (Koposov et al. 2015a; Walker et al. 2016): Hor 1 and Ret 2 are clear candidates, whereas Tuc 2 and Gru 1 seem only marginally consistent with a Magellanic origin.

Table 1. Parameters of the newly discovered dwarfs considered in this paper, together with their LMC ‘association index’ for either first or second pericentre passage, as defined in Section 3.4. Columns 8 and 9 list association indices (our proxy for probabilities) computed using positions alone; columns 10 and 11 also include also radial velocity data. We list the V -band absolute magnitude, stellar mass, galactocentric coordinates (l , b), measured heliocentric radial velocity V_{\odot} , and heliocentric distance D_{\odot} of each satellite, taken from the following references: [1] Koposov et al. 2015b, [2] Drlica-Wagner et al. 2015, [3] Martin et al. 2015, [4] Laevens et al. 2015, [5] Kim & Jerjen 2015, [6] Kim et al. 2015a, [7] Torrealba et al. 2016, [8] McConnachie 2012, [9] Simon et al. 2015, [10] Koposov et al. 2015a, [11] Kirby et al. 2015, [12] Walker et al. 2016 and [13] Martin et al. 2016). For cases without estimates of M_* , we derive it from their listed V -band magnitudes assuming a mass-to-light ratio $\gamma = 2$ in solar units. Dwarfs are grouped according to their association index with the Clouds at first pericentre, using only their distance and position on the sky (column 8). The main two groups include ‘likely candidates’ and ‘unlikely candidates’, according to whether their probabilities are above or below 20 per cent. The final group lists those that were discarded from the analysis, either because their position on the sky is such that the probability of LMC association is remote, or because they are considered star clusters, and not dwarf galaxies.

Name	M_V (mag)	M_* [$10^3 M_{\odot}$]	l (deg)	b (deg)	V_{\odot} (km s^{-1})	D_{\odot} (kpc)	a_p 1st per	a_p 2nd per	a_{pv} 1st per	a_{pv} 2nd per	Refs.
LMC	−18.1	1.5×10^6	280.5	−32.9	262.2	51	0.95	0.94	0.99	0.98	[8]
SMC	−16.8	4.6×10^5	302.8	−44.3	145.6	64	0.68	0.45	0.86	0.78	[8]
Hor 1	−3.4	1.96	270.9	−54.7	112.8 ± 2.5	79	0.60	0.26	0.68	0.32	[1],[10]
Hor 2	−2.6	2.47	262.5	−54.1	–	26	0.51	0.18	–	–	[5]
Eri 3	−2.0	0.54	274.3	−59.6	–	87	0.45	0.16	–	–	[1]
Tuc 5	−1.6	9.	316.3	−51.9	–	55	0.38	0.16	–	–	[2]
Tuc 4	−3.5	4.	313.3	−55.3	–	48	0.34	0.13	–	–	[2]
Phx 2	−2.8	1.13	323.3	−60.2	–	83	0.28	0.18	–	–	[1]
Ret 3	−3.3	13.0	273.9	−45.6	–	92	0.26	0.04	–	–	[2]
Tuc 2	−4.4	4.9	327.9	−52.8	$−129.1 \pm 3.5$	69	0.21	0.11	0.10	<0.01	[1],[12]
Ret 2	−2.7	1.0	265.9	−49.6	62.8 ± 0.5	30	0.11	0.02	0.03	<0.01	[1],[9],[10]
Gru 2	−3.9	5.0	351.1	−51.9	–	53	0.07	0.04	–	–	[2]
Peg 3	−4.1	7.46	69.8	−41.8	–	26	0.05	0.23	–	–	[6]
Tuc 3	−2.4	2.0	315.4	−56.2	–	25	0.02	<0.01	–	–	[2]
Gru 1	−3.4	1.96	338.6	−58.8	$−140.5 \pm 2.0$	120	<0.01	0.01	0.0	<0.01	[1],[12]
Pic 1	−3.1	1.5	257.1	−40.4	–	114	0.01	0.0	–	–	[1]
Cra 2	−8.2	2.25	283.9	+41.9	–	118	<0.01	0.20	–	–	[7]
Dra 2	−2.9	2.47	98.3	+42.9	$−347.6 \pm 1.8$	20	<0.0	<0.01	0.0	<0.01	[4],[13]
Hy II	−4.8	7.1	295.6	+30.5	303.1 ± 1.4	134	0.0	0.06	0.0	0.06	[3],[11]
Eri 2**	−6.6	37.3	249.4	51.4	–	380	0.0	0	–	–	[1]
Sag 2**	−5.2	2.47	189.0	−22.9	–	67	–	–	–	–	[4]
Ind 1**	−3.5	2.1	347.3	−42.6	–	100	–	–	–	–	[1]
Col 1**	−4.5	18.0	231.6	−28.9	–	182	–	–	–	–	[2]

More stringent constraints may be obtained by combining the results from Figs 1 and 3, since membership to the LMC group is only likely for systems in narrow regions of the four-dimensional space drawn by (i) position on the sky (l , b); (ii) radial velocity V_r , and (iii) Galactocentric distance r_{GC} . We illustrate this in Fig. 4, where we plot the distance and radial velocity of all LMCa particles whose positions on the sky fall within 5° of each individual dwarf. (We have explicitly checked that none of our results would significantly change if we use a different angular distance around each dwarf, for instance 10° instead of the fiducial 5° ; see also S11.)

The top two panels on the left of Fig. 4 are meant to illustrate the analysis procedure. For the case of the LMC (top left), most particles in the LMCa sub-halo are, by construction (Section 2.2), at the observed location and radial velocity of the LMC (shown with a blue square). The SMC panel illustrates that most LMCa particles selected in that direction of the sky ($b = -44.3^\circ$, $l = 302.8^\circ$) are at ~ 58 kpc from the Galactic Centre and have, on average, a radial velocity of ~ 5 km s^{-1} , which is in excellent agreement with the observed SMC values (blue square).

The red vertical bands in the panels of Fig. 4 indicate a (generous) 20 per cent uncertainty in the distance estimate to each dwarf; its intersection with LMCa particles is used to draw the velocity histograms in the right-hand side of each panel. Coincidence between the velocity of the blue square and the histogram indicates that the

observed velocity is not unexpected in a scenario where the dwarf originates from a disrupted LMC group. The velocity histograms may therefore be used to ‘predict’ the radial velocity of dwarfs for which kinematic data are not yet available, *assuming* a Magellanic origin.

As may be seen from Fig. 4, and not surprisingly, the SMC passes these tests handily, making its association with the LMC quite likely. On the other hand, the probability of association of a dwarf like Fornax is quite remote. Most debris in that direction of the sky are at much closer distances, and the little that overlaps in distance with Fornax (two particles) has a rather high positive radial velocity, quite unlike that observed. This illustrates the arguments used by S11 to exclude an LMC association not only for Fornax but also for all other Galactic satellites known at that time in case of first infall.

The six ‘new dwarfs’ with kinematic data are shown in the bottom two rows of Fig. 4. From this comparison, we conclude that Dra 2 has little chance of LMC association. Likewise, Ret 2, Tuc 2, and Gru 1 have velocities only marginally consistent with a Magellanic relation. Hy II, on the other hand, has the correct radial velocity for its distance, despite its large angular separation from the LMC, at the far northern edge region of the leading stream. The only clear candidate for Magellanic association is Hor 1, which is well within the expected velocity–distance range at its location.

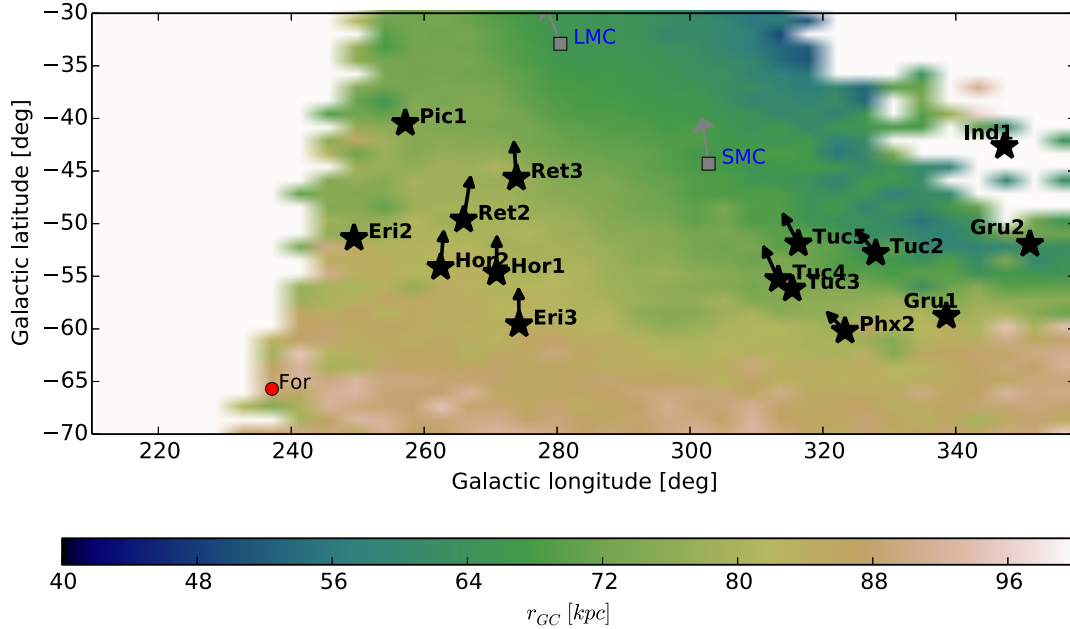


Figure 2. Zoom-in of the area just south of the Clouds outlined by the dashed magenta box in Fig. 1. This area samples the trailing arm of the LMCa tidal debris, and contains the new dwarfs discovered in the Dark Energy Survey (DES). Col 1 is the only DES dwarf located far away from the stream (not shown). Note also that Ind 1 has now been shown to be a star cluster (Kim et al. 2015b). The LMC and the SMC are shown as grey squares; red circles are previously known Galactic satellites; new dwarfs are shown by starred symbols. The arrows indicate the expected tangential motion of those satellites, assuming that they were associated with the Clouds (see Section 3.6). Arrows are shown only for systems deemed likely Magellanic satellite candidates in a first pericentre passage scenario (see the text for more details).

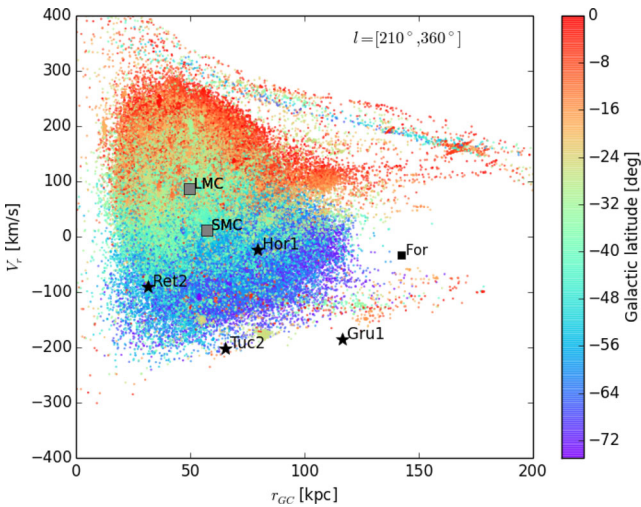


Figure 3. Galactocentric distance r_{GC} versus radial velocity V_r for LMCa particles at first pericentre, colour-coded by Galactic latitude b ($-80^\circ < b < 0^\circ$; see colour bar on right). For clarity, we only show the Galactic longitude range $l = [210^\circ, 360^\circ]$, which encompasses most of the LMCa material in Fig. 1. Note the correlation between latitude and radial velocity, with the leading arm having already passed through pericentre (positive V_r) and the trailing material still approaching the Galaxy with $V_r < 0$. As before, the LMC and SMC are shown with grey squares and other previously known dwarfs in this region of the sky are marked with black squares; new dwarfs with measured kinematics are shown with black-starred symbols. The little overlap between Fornax, Gru 1 and Tuc 2 and the LMCa debris implies a low probability of prior association between these dwarfs and the LMC, assuming first infall. Hor 1 is the dwarf most likely to have had a Magellanic association.

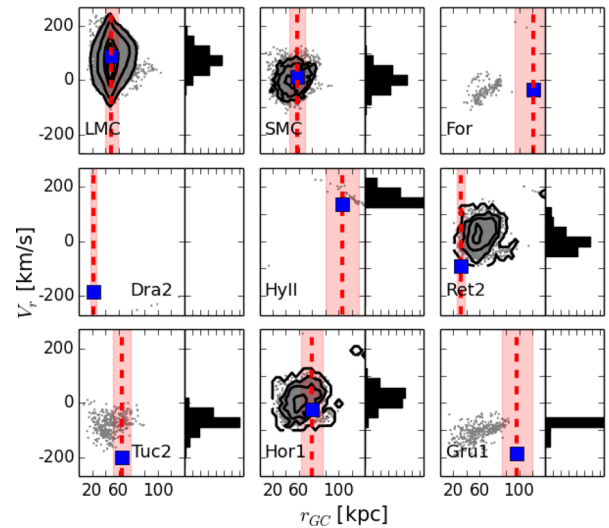


Figure 4. Galactocentric distance versus radial velocity for LMCa particles within 5° from each observed dwarf (blue squares), as labelled. Particles with r_{GC} within 20 percent of the observed distance fall within the red-shaded area, and are used to ‘predict’ the radial velocity expected for LMC association (see black velocity histograms on the right of each panel). The top three panels are meant to illustrate the procedure for well-studied systems. The LMC sits at the middle of the distribution by construction. The SMC is a likely LMC satellite; Fornax is not. The bottom two rows show the newly discovered dwarfs for which kinematic measurements are available. Only Hy II and Hor 1 show velocities consistent with those expected for prior association with the LMC.

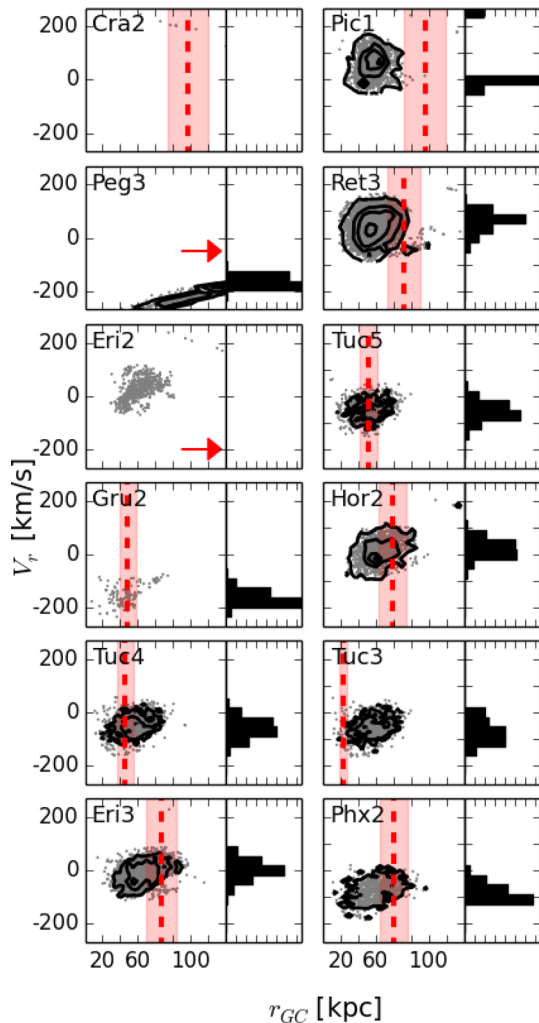


Figure 5. Same as Fig. 4 but for the new dwarfs with no measured V_r . The Galactocentric distances for Pic 1, Eri 2 and Tuc 3 seem inconsistent with the distances measured for the LMCa debris around their positions on the sky (red arrows indicate that the measured distances for Eri 2 and Peg 3 fall outside the distance range plotted). On the other hand, Ret 3, Hor 2 and several of the Tucanas show high chance of association, at least based on their positions and distances alone.

3.3 Predicted radial velocities for candidate Magellanic satellites

We can use the procedure described in the previous subsection to predict the radial velocities that the remaining ‘new dwarfs’ would have if they were truly Magellanic satellites. We show this in Fig. 5, which lists dwarfs in order of decreasing Galactic latitude. Inspection of individual panels suggests some preliminary conclusions. The Galactocentric distances measured for Pic 1 and Eri 2 seem inconsistent with previous association with the LMC. Cra 2 is in the same category, given the very little overlap with the edge of the leading arm of the stream. Aside from those three cases, all other dwarfs show some degree of overlap in the (l, b) - r_{GC} plane with the LMCa debris. For the latter, the black histograms in Fig. 5 show their expected radial velocities for a Magellanic origin. We summarize these predictions in Table 3, together with uncertainties derived from the interquartile velocity range of the histograms in Fig. 5.

3.4 Probability of LMC association

The discussion of Fig. 4 and 5 suggests that, for each dwarf, the likelihood of prior LMC association scales with the total number of LMCa particles that match its sky position, distance, and radial velocity, compared with the number of particles of the main halo that satisfy the same constraints.

An ‘association index’ may thus be computed for each dwarf by estimating, at its observed position (and velocity, when available), the fraction of all particles contributed by LMCa. We take this to be given by the fraction of LMCa particles in a small 3D (or 4D, if radial velocities are included) volume centred on the dwarf. In practice, we use a sphere of radius 10 kpc for the estimate³; if n_{LMCa} is the number of LMCa particles in that volume and n_{halo} is the number corresponding to the main halo, we define the position-based association index as $a_p = f_m n_{\text{LMCa}} / (f_m n_{\text{LMCa}} + n_{\text{halo}})$. Here, we take into account that our LMC analogue has lower mass than expected by increasing the weight of each LMCa particle by a factor of $f_m = 8.3$ (see Section 2.1). For simplicity, the host halo is modelled as a spherical, isotropic Navarro–Frenk–White (Navarro, Frenk & White 1996, 1997) profile with virial mass $1.6 \times 10^{12} M_\odot$ and concentration $c = 15$. Association indexes are listed in Table 1 for all newly discovered dwarfs.

For dwarfs with measured radial velocities, we can compute a position–velocity association index by comparing the measured V_r of the dwarf with the distribution of velocities for LMCa and host halo particles in the same 10 kpc-radius sphere. Because of small number statistics, we approximate each distribution by a Gaussian (G_{LMCa} and G_{halo} , respectively) centred on the mean radial velocity and with dispersion given by the rms velocity of each group of particles. The relative weight of each Gaussian is proportional to $f_m n_{\text{LMCa}}$ and n_{halo} , respectively. The position–velocity association index is then computed by comparing the heights of these two distributions at the dwarf radial velocity, $a_{pv} = G_{\text{LMCa}}(V_r) / (G_{\text{LMCa}}(V_r) + G_{\text{halo}}(V_r))$. These indexes are listed in columns 10 and 11 of Table 1.

The results are shown in Table 1, where we list all ‘new dwarfs’, as well as their assigned association indices, with and without velocity information. As discussed before, aside from the SMC, the procedure ranks Hor 1 as the best candidate for a true Magellanic satellite when considering satellites with or without radial velocities. Of systems without kinematic data, Hor 2, Eri 3, and Tuc 5 are the best candidates, but this could certainly change when radial velocities become available. An example of the importance of kinematic information is provided by Ret 2, whose association index drops substantially (from ~ 0.11 to 0.02) when adding its radial velocity to the analysis (assuming first pericentre).

We shall hereafter retain as ‘candidate Magellanic satellites’ systems with position association index $a_p > 0.2$. The list of candidates is quite short: only 8 systems of the 20 new dwarfs make the cut in the case of position-only information: Hor 1, Hor 2, Eri 3, Tuc 5, Tuc 4, Phx 2, Ret 3, and Tuc 2.

Our results are in agreement with the previous work although, because of the different metrics used to quantify probability of association in each paper, a quantitative comparison is not possible. However, comparing our rank-ordered list to the most likely candidates reported by Deason et al. (2015) and Jethwa et al. (2016), we find that all of their candidates are recovered by our analysis, with the exception of Ret 2, which, according to our results, has a

³ We have checked that none of our conclusions change when choosing radii of 5 or 20 kpc for this exercise.

radial velocity that is too negative at its position. It is possible that allowing for variations in the LMC orbit, as explored in Jethwa et al. (2016), might make it easier to accommodate the measured velocity of Ret 2. However, for the particular configuration we explore here it seems rather unlikely (even its position index is only $a = 0.11$).

3.5 Second pericentre

The above procedure also allows us to explore the sensitivity of our findings to our assumption that the LMC is on first approach. We do this by performing the same analysis but using the LMCa data at second pericentre (t_{2p}), after updating the Galactic coordinate system transformation described in Section 2.2. The new association indices are also listed in Table 1.

Because of the tidal disruption of the LMCa, the association indices are smaller on the second pericentre due to the lower density of the debris as a result of a more extended distribution on the sky. In general, however, there is a strong correlation between the indices at both pericentres, so our conclusions seem only weakly dependent on the assumption of first infall. The increase in a_p is most notable in the cases of Peg 3 and Cra 2, whose values jump from 0.05 and <0.01 in a first pericentre passage to 0.23 and 0.20, respectively, when considering the second pericentre passage.

The reason for this, in the case of Peg 3, is that it sits at the very far edge of the ‘trailing arm’ of the tidal stream. Although its distance and velocity are consistent with an LMC association, at first infall there are only a few particles at that sky location and its probability is quite low. When the Clouds are in a second passage, several particles accumulate near the apocentre of the LMCa orbit, not far from where Peg 3 is, increasing substantially its likelihood of association. Similarly, Cra 2 is at the tip of the leading arm of the stream, a position that is much more heavily populated after the Clouds have completed one full orbit around the Galaxy. Hy II is also near Cra 2 and shows a higher association index in a second passage. However, the density of the stream even at t_{2p} is too low at that distance compared to the host halo, resulting in a small increase on association index (0.06 at second pericentre compared to 0 for the first).

3.6 Proper motions: conclusive proof of Magellanic origin

Ultimately, the most compelling evidence for LMC association will come from the proper motions of the new dwarfs. This is because all material associated with the LMC before infall is expected to retain the direction of its orbital angular momentum. In other words, to first order, Galactic tides are not expected to torque the LMC or its debris away from their original orbital plane.

We show this in Fig. 6, where we plot the *direction* of the orbital angular momentum of LMCa particles at first pericentre. The innermost and outermost isodensity contours enclose 5 and 95 per cent of all LMCa particles, respectively, and are centred at the location of the LMC orbital pole (central grey square). The other grey square (at $b = -20^\circ$ and $l = 175^\circ$) corresponds to the SMC, and is consistent with its assumed association with the LMC.

We also show with starred symbols in Fig. 6 the orbital angular momentum direction *predicted* for each of the ‘candidate Magellanic satellites’ (i.e. those with $a_p > 0.2$) at first pericentre *assuming* that they were associated with the LMC. This is computed as the median l and b of the orbital poles of all LMCa particles with matching sky position and Galactocentric distance (i.e. the particles that fall into the red-shaded regions of each panel in Fig. 4 and 5).

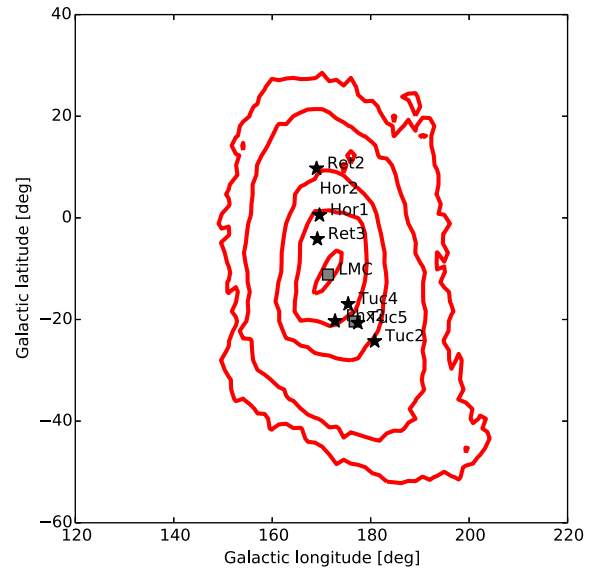


Figure 6. Sky coordinates of the orbital poles (i.e. the direction of the orbital angular momentum) of particles associated with LMCa. Contours show constant density lines for the distribution of all LMCa. Symbols correspond to the orbital poles estimated for new dwarf galaxies deemed likely candidate Magellanic satellites at first pericentre, as labelled. These estimates are based on the particles in the stream that are close in the sky and that lie at distances within 20 per cent of the measured values (see red-shaded regions in Figs. 4 and 5). The common infall scenario preserves the coherence of the orbital plane, resulting in a tight distribution of the orbital poles in a well-defined region of the sky.

We list in Table 2, for each Magellanic candidate, the coordinates of the predicted orbital angular momentum unit vector, in a Cartesian system where the Z-axis is perpendicular to the Galactic disc, the X-axis points away from the Sun and the Y-axis is defined such that we get a right-handed system. Uncertainties correspond to the rms values from the individual LMCa particles used for each dwarf.

Assuming a radial velocity (for those without a measurement), this is equivalent to predicting the tangential motion of each dwarf, which we also list in Table 3. The predicted projected velocities are shown with arrows in Fig. 2. Table 2 may therefore be used to evaluate the hypothesis of prior LMC association for these dwarfs once proper motions for these objects become available.

4 SUMMARY

We have used a Λ CDM cosmological N -body simulation of the formation of an MW-sized halo to investigate which of the 20 newly discovered Galactic satellites in the DES, Pan-STARRS, SMASH, and ATLAS surveys might have been associated with the Magellanic Clouds before infall. Our study extends that of S11, which used a massive sub-halo with orbital parameters that closely match those of the LMC (an LMC analogue: LMCa) and tracked the position and velocity of its constituent particles at the first and second pericentric passages. This enables the likelihood of LMC association to be assessed by checking whether individual dwarfs lie in a region of phase space populated by debris from the disrupting LMC sub-halo.

On the basis of that analysis, S11 concluded that, except for the SMC, none of the other 26 Galactic satellites known at the time had positions and velocities consistent with a Magellanic origin. That was the first study to investigate a possible Magellanic association by using all of the available phase-space information in a fully

Table 2. Cartesian components of the direction (average) of the angular momentum of the LMCa particles near each Magellanic candidate dwarf, according to the discussion of Section 3.4. Only dwarfs with association index $a_p > 0.2$ in Table 1 are listed here. All vectors are normalized to have modulus unity. For each dwarf, we list the results for the first (top row) and/or second (bottom row) pericentre passage. The bottom group includes dwarfs that are only likely Magellanic candidates at second pericentre. Because the LMC is in a nearly polar orbit, the angular momentum of all material associated with it points in all cases in the $-X$ direction (i.e. to the Sun from the Galactic Centre).

Name	time	j_x	j_y	j_z
LMC	t_{1p}	-0.97 ± 0.03	0.14 ± 0.07	-0.19 ± 0.10
	t_{2p}	-0.97 ± 0.03	0.14 ± 0.06	-0.18 ± 0.09
	Observed	-0.97 ± 0.01	0.14 ± 0.02	-0.18 ± 0.03
SMC	t_{1p}	-0.92 ± 0.05	0.04 ± 0.10	-0.35 ± 0.08
	t_{2p}	-0.90 ± 0.05	0.05 ± 0.17	-0.38 ± 0.10
	Observed	-0.91 ± 0.05	0.08 ± 0.11	-0.39 ± 0.09
Hor 1	t_{1p}	-0.98 ± 0.05	0.18 ± 0.10	-0.04 ± 0.09
	t_{2p}	-0.95 ± 0.19	0.30 ± 0.50	-0.10 ± 0.36
Hor 2	t_{1p}	-0.97 ± 0.02	0.24 ± 0.09	-0.03 ± 0.08
	t_{2p}	-0.73 ± 0.18	-0.48 ± 0.46	0.49 ± 0.28
Eri 3	t_{1p}	-0.99 ± 0.07	0.16 ± 0.10	-0.04 ± 0.07
	t_{2p}	-0.94 ± 0.20	0.31 ± 0.61	-0.14 ± 0.37
Tuc 5	t_{1p}	-0.93 ± 0.03	0.12 ± 0.13	-0.34 ± 0.05
	t_{2p}	-0.90 ± 0.04	0.09 ± 0.14	-0.42 ± 0.08
Tuc 4	t_{1p}	-0.95 ± 0.03	-0.06 ± 0.17	-0.30 ± 0.06
	t_{2p}	-0.93 ± 0.03	0.13 ± 0.12	-0.28 ± 0.08
Phx 2	t_{1p}	-0.93 ± 0.02	0.13 ± 0.10	-0.34 ± 0.04
	t_{2p}	-0.92 ± 0.02	0.13 ± 0.13	-0.37 ± 0.05
Ret 3	t_{1p}	-0.98 ± 0.02	0.18 ± 0.07	-0.11 ± 0.08
	t_{2p}	-0.94 ± 0.19	0.28 ± 0.50	-0.15 ± 0.44
Tuc2	t_{1p}	-0.90 ± 0.03	-0.18 ± 0.22	-0.38 ± 0.06
	t_{2p}	-0.87 ± 0.03	0.08 ± 0.16	-0.49 ± 0.06
Peg 3	t_{2p}	-0.97 ± 0.02	0.25 ± 0.17	-0.03 ± 0.12
Cra 2	t_{2p}	-0.97 ± 0.08	0.12 ± 0.17	0.20 ± 0.16

cosmological context. Extending this study to the newly discovered dwarfs yields the following conclusions, assuming that the LMC is at first pericentric passage.

(i) We first eliminate four systems from our analysis. Sag 2, Eri 2, and Col 1 lie too far outside the LMCa footprint for their association

with the LMC to be plausible. In addition, Ind 1 has recently been reclassified as a star cluster.

(ii) For the rest of the systems, a quantitative ‘association index’ may be defined by the ratio of LMCa particles to those of the main halo at the position (a_p) of each dwarf or using its position and radial velocity (a_{pv}). We deem candidate Magellanic satellites dwarfs whose position association index exceeds $a_p = 0.2$.

(iii) Of the six systems with available distances and radial velocities, only two (Hor 1 and Tuc 2) are candidate Magellanic satellites. Radial velocity information strengthens the likelihood of association of Hor 1, but decreases that of Tuc 2 and of all other four (Ret 2, Gru 1, Dra 2, and Hy II). Ret 2 is marginally consistent in position, but its radial velocity is rather unlikely for Magellanic association. Dra 2 is too far off the LMCa first-pericentre footprint. Hy II has the right distance *and* radial velocity, but its association index is small, given its position at the thinly populated, very far end of the LMCa leading tidal arm.

(iv) Of the remaining 11 systems with only sky positions and distances, our analysis retains 6 of them with $a_p > 0.2$ (Hor 2, Eri 3, Tuc 5, Tuc 4, Phx 2, and Ret 3). For these candidates, we use the velocity of the associated LMCa particles to *predict* their radial velocities, assuming a Magellanic origin.

(v) Aside from radial velocities, the most telling evidence of a potential LMC association would be provided by proper motions. These constrain the direction of the orbital angular momentum of each dwarf, which must roughly coincide with that of the LMC. We use this result to predict proper motions for all newly discovered satellites, again assuming a Magellanic origin. The radial and tangential velocity predictions could be used to reassess the hypothesis of a possible Magellanic association once kinematic data become available.

Our conclusions are insensitive to our choice of first or second pericentre for the LMC, in the sense that the association indices of most dwarfs computed at either time are strongly correlated. Because the LMCa debris spreads out to cover a larger volume in phase space at second pericentre, the association indices of four extra systems, computed using positions alone, are lifted above 0.2: Cra 2 and Peg 3. Velocity information would be particularly welcome in these two cases to verify a possible Magellanic origin.

Table 3. Predicted Galactocentric radial and tangential velocity for Magellanic candidate dwarfs under the assumption of association with the Clouds. As before, only dwarfs with association index $a_p > 0.20$ in Table 1 are listed here. We show the median and 25–75 per cent percentiles in the case of the first (columns 2–4) and second (columns 5–7) pericentre passages. The last column shows the galactocentric radial velocity for the six dwarfs with measured kinematics. The bottom group includes dwarfs that are only likely Magellanic candidates at second pericentre.

Name	V_r^{pred} (km s^{-1})	V_l^{pred} 1st per.	V_b^{pred} 1st per.	V_r^{pred} 2nd per.	V_l^{pred} 2nd per.	V_b^{pred} 2nd per.	V_r^{obs} (km s^{-1})
Hor 1	19_{+23}^{-22}	5_{+27}^{-30}	330_{+17}^{-25}	23_{+22}^{-17}	1_{+73}^{-38}	266_{+30}^{-200}	-23.2
Hor 2	20_{+25}^{-10}	44_{+26}^{-22}	326_{+19}^{-17}	30_{+36}^{-26}	70_{+13}^{-36}	56_{+216}^{-21}	
Eri 3	5_{+23}^{-23}	-57_{+78}^{-26}	323_{+22}^{-26}	22_{+31}^{-39}	8_{+65}^{-45}	252_{+28}^{-200}	
Tuc 5	-58_{+26}^{-21}	-225_{+27}^{-24}	272_{+23}^{-28}	-50_{+28}^{-27}	-245_{+30}^{-17}	221_{+32}^{-21}	
Tuc 4	-58_{+24}^{-21}	-213_{+26}^{-25}	297_{+23}^{-25}	-43_{+18}^{-28}	-221_{+28}^{-24}	256_{+24}^{-24}	
Phx 2	-90_{+30}^{-6}	-273_{+34}^{-8}	180_{+30}^{-5}	-58_{+21}^{-24}	-237_{+18}^{-18}	161_{+25}^{-24}	
Ret 3	72_{+16}^{-32}	36_{+21}^{-15}	326_{+25}^{-19}	38_{+26}^{-23}	-8_{+86}^{-44}	244_{+35}^{-180}	
Tuc2	-67_{+20}^{-14}	-261_{+30}^{-18}	202_{+32}^{-34}	-73_{+29}^{-19}	-265_{+23}^{-18}	133_{+33}^{-22}	-201.5
	–	–	–	-73_{+29}^{-19}	-265_{+23}^{-18}	133_{+33}^{-22}	-201.5
Peg 3	–	–	–	-110_{+8}^{-16}	-16_{+10}^{-9}	-131_{+7}^{-8}	
Cra 2	–	–	–	108_{+36}^{-21}	-156_{+49}^{-36}	228_{+16}^{-42}	

Our main conclusion is therefore that few of the newly discovered dwarfs are definitely associated with the LMC. This is not entirely unexpected. The simple scaling argument of Sales et al. (2013) suggests that the fraction of all Galactic satellites associated with the Clouds should be close to the ratio of the stellar mass of the LMC and the MW, i.e. ~ 5 per cent. Given that we now have identified a total ~ 46 dwarfs within 300 kpc from the Galactic Centre (excluding the LMC/SMC pair), only two to three should, in principle, be associated with the Clouds. So far our analysis seems consistent with this expectation. Accurate radial velocities and proper motions are needed to accept/reject the hypothesis of association between these dwarfs and the LMC. Confirming the existence of multiple Magellanic satellites would provide a wonderful confirmation of the hierarchical nature of galaxy formation predicted by the current cosmological paradigm.

ACKNOWLEDGEMENTS

We thank the referee for a constructive and detailed report that helped to significantly improve the first version of this paper. The authors thank Marius Cautun for helpful discussions. NK is supported by the NSF CAREER award 1455260. This research was supported in part by the National Science Foundation under Grant No. NSF PHY11-25915 and by the hospitality of the Kavli Institute for Theoretical Physics at the University of California, Santa Barbara.

REFERENCES

- Bechtol K. et al., 2015, *ApJ*, 807, 50
 Behroozi P. S., Wechsler R. H., Conroy C., 2013, *ApJ*, 770, 57
 Besla G., Kallivayalil N., Hernquist L., Robertson B., Cox T. J., van der Marel R. P., Alcock C., 2007, *ApJ*, 668, 949
 Boylan-Kolchin M., Springel V., White S. D. M., Jenkins A., Lemson G., 2009, *MNRAS*, 398, 1150
 Boylan-Kolchin M., Besla G., Hernquist L., 2011, *MNRAS*, 414, 1560
 Boylan-Kolchin M., Bullock J. S., Sohn S. T., Besla G., van der Marel R. P., 2013, *ApJ*, 768, 140
 D’Onghia E., Fox A. J., 2016, *ARA&A*, 54, 363
 D’Onghia E., Lake G., 2008, *ApJ*, 686, L61
 Deason A. J., Wetzel A. R., Garrison-Kimmel S., Belokurov V., 2015, *MNRAS*, 453, 3568
 Dehnen W., Binney J. J., 1998, *MNRAS*, 298, 387
 Diemand J., Moore B., Stadel J., 2004, *MNRAS*, 352, 535
 Drlica-Wagner A. et al., 2015, *ApJ*, 813, 109
 Gao L., White S. D. M., Jenkins A., Stoehr F., Springel V., 2004, *MNRAS*, 355, 819
 Garrison-Kimmel S., Boylan-Kolchin M., Bullock J. S., Lee K., 2014, *MNRAS*, 438, 2578
 Jethwa P., Erkal D., Belokurov V., 2016, *MNRAS*, 461, 2212
 Kallivayalil N., van der Marel R. P., Alcock C., Axelrod T., Cook K. H., Drake A. J., Geha M., 2006, *ApJ*, 638, 772 (K06)
 Kallivayalil N., van der Marel R. P., Besla G., Anderson J., Alcock C., 2013, *ApJ*, 764, 161
 Kennedy R., Frenk C., Cole S., Benson A., 2014, *MNRAS*, 442, 2487
 Kim D., Jerjen H., 2015, *ApJ*, 808, L39
 Kim D., Jerjen H., Mackey D., Da Costa G. S., Milone A. P., 2015a, *ApJ*, 804, L44
 Kim D., Jerjen H., Milone A. P., Mackey D., Da Costa G. S., 2015b, *ApJ*, 803, 63
 Kirby E. N., Simon J. D., Cohen J. G., 2015, *ApJ*, 810, 56
 Komatsu E. et al., 2009, *ApJS*, 180, 330
 Koposov S. E. et al., 2015a, *ApJ*, 811, 62
 Koposov S. E., Belokurov V., Torrealba G., Evans N. W., 2015b, *ApJ*, 805, 130
 Laevens B. P. M. et al., 2015, *ApJ*, 813, 44
 Li Y., White S. D. M., 2008, *MNRAS*, 384, 1459
 Lynden-Bell D., Lynden-Bell R. M., 1995, *MNRAS*, 275, 429
 Martin N. F. et al., 2015, *ApJ*, 804, L5
 Martin N. F. et al., 2016, *MNRAS*, 458, L59
 McConnachie A. W., 2012, *AJ*, 144, 4
 McMillan P. J., 2016, preprint ([arXiv:e-prints](https://arxiv.org/abs/1608.00147))
 Moster B. P., Naab T., White S. D. M., 2013, *MNRAS*, 428, 3121
 Navarro J. F., Frenk C. S., White S. D. M., 1996, *ApJ*, 462, 563
 Navarro J. F., Frenk C. S., White S. D. M., 1997, *ApJ*, 490, 493
 Nidever D. L., Majewski S. R., Butler Burton W., Nigra L., 2010, *ApJ*, 723, 1618
 Sales L. V., Navarro J. F., Abadi M. G., Steinmetz M., 2007, *MNRAS*, 379, 1464
 Sales L. V., Navarro J. F., Cooper A. P., White S. D. M., Frenk C. S., Helmi A., 2011, *MNRAS*, 418, 648 (S11)
 Sales L. V., Wang W., White S. D. M., Navarro J. F., 2013, *MNRAS*, 428, 573
 Shattow G., Loeb A., 2009, *MNRAS*, 392, L21
 Simon J. D. et al., 2015, *ApJ*, 808, 95
 Smith M. C. et al., 2007, *MNRAS*, 379, 755
 Spergel D. N. et al., 2003, *ApJS*, 148, 175
 Springel V., Yoshida N., White S. D. M., 2001, *New Astron.*, 6, 79
 Springel V. et al., 2008a, *Nature*, 456, 73
 Springel V. et al., 2008b, *MNRAS*, 391, 1685
 Torrealba G., Koposov S. E., Belokurov V., Irwin M., 2016, *MNRAS*, 459, 2370
 Tully R. B. et al., 2006, *AJ*, 132, 729
 van der Marel R. P., Kallivayalil N., 2014, *ApJ*, 781, 121
 Vogelsberger M. et al., 2014, *Nature*, 509, 177
 Walker M. G. et al., 2016, *ApJ*, 819, 53
 Wang W., Sales L. V., Henriques B. M. B., White S. D. M., 2014, *MNRAS*, 442, 1363
 Wetzel A. R., Deason A. J., Garrison-Kimmel S., 2015, *ApJ*, 807, 49
 Wheeler C., Oñorbe J., Bullock J. S., Boylan-Kolchin M., Elbert O. D., Garrison-Kimmel S., Hopkins P. F., Kereš D., 2015, *MNRAS*, 453, 1305
 Yozin C., Bekki K., 2015, *MNRAS*, 453, 2302

This paper has been typeset from a $\text{\TeX}/\text{\LaTeX}$ file prepared by the author.